Topological and spectral properties of random digraphs

C. T. Martínez-Martínez,[1] J. A. Méndez-Bermúdez,[2,3] and José M. Sigarreta[1]

[1]*Facultad de Matemáticas, Universidad Autónoma de Guerrero, Carlos E. Adame 5, Col. La Garita, Acapulco, Guerrero, Mexico*

[2]*Instituto de Física, Benemérita Universidad Autónoma de Puebla, Puebla 72570, Mexico*

[3]*Escuela de Física, Facultad de Ciencias, Universidad Nacional Autónoma de Honduras, Honduras*

(Received 10 November 2023; revised 25 April 2024; accepted 31 May 2024; published 12 June 2024)

We investigate some topological and spectral properties of Erdős-Rényi (ER) random digraphs of size n and connection probability p, $D(n, p)$. In terms of topological properties, our primary focus lies in analyzing the number of nonisolated vertices $V_x(D)$ as well as two vertex-degree-based topological indices: the Randić index $R(D)$ and sum-connectivity index $\chi(D)$. First, by performing a scaling analysis, we show that the average degree $\langle k\rangle$ serves as a scaling parameter for the average values of $V_x(D)$, $R(D)$, and $\chi(D)$. Then, we also state expressions relating the number of arcs, largest eigenvalue, and closed walks of length 2 to (n, p), the parameters of ER random digraphs. Concerning spectral properties, we observe that the eigenvalue distribution converges to a circle of radius $\sqrt{np(1-p)}$. Subsequently, we compute six different invariants related to the eigenvalues of $D(n, p)$ and observe that these quantities also scale with $\sqrt{np(1-p)}$. Additionally, we reformulate a set of bounds previously reported in the literature for these invariants as a function (n, p). Finally, we phenomenologically state relations between invariants that allow us to extend previously known bounds.

DOI: 10.1103/PhysRevE.109.064306

I. INTRODUCTION

In recent years, there has been a significant increase in the use of graphs to represent complex systems in various fields, including computer science, engineering, biology, and social sciences [1–5]. This growing trend can be attributed to the effectiveness of capturing the properties of complex systems through graphs, where the vertices represent the agents of the system and the edges reflect their interactions. This, in turn, opens the door to the analysis of complex systems through various mathematical techniques coming mainly from graph theory.

The study of the properties of graphs covers many aspects, focusing mainly on topological and spectral properties. One of the ways to study and characterize these properties is through their topological descriptors, such as degree distribution, clustering coefficient, eigenvector centrality, and, more recently, topological indices [6–9].

Although many studies have been carried out with highly relevant results about the topological and spectral properties of graphs, most of them focus on graphs whose edges do not have a specific direction, in which the connection between two vertices is symmetric and bidirectional (undirected graphs). However, in several cases, it is mandatory to incorporate the direction of the information flow when considering the modeling of real-world systems. This is indeed the case when considering food webs [10–12], neural networks [13–15], genetic regulation [16], chemical networks [17,18], fluid flows [19,20], or financial networks [21], among many other relevant applications. In these scenarios, it is crucial to capture the orientation of the connections so that the systems are represented by directed networks, commonly known as digraphs. Consequently, there is a specific interest in exploring the properties of directed graphs.

A digraph or directed graph is a mathematical structure denoted as $D = (V, E)$, where V represents a finite set of n elements called vertices or nodes and $E \subset V \times V$ comprises m directed edges (also called arcs) connecting vertices.

Topological properties delve into the fundamental structural properties of digraphs, including connectivity, accessibility, cycles, and paths. In this line, applying topological indices based on vertex degrees to characterize and analyze the topological properties of graphs has been a widely used approach. The concept of an index based on vertex degrees originates in chemical graph theory, which uses graph theory to study the properties of chemical compounds by representing them as graphs, where atoms are vertices and bonds are edges. The vertex-degree-based (VDB) topological indices quantify some aspects of the topology of the graph in relation to the degrees of its vertices. In a general formulation, a VDB topological index can be expressed as [22]

$$\mathrm{TI} = \mathrm{TI}(G) = \sum_{i\sim j} f(k_i, k_j), \tag{1}$$

where the summation extends over all pairs of adjacent vertices, denoted as i and j, within the molecular graph G, k_i is the degree of the vertex i, and $f(k_i, k_j)$ represents a function tailored to the specific topological property under investigation. Since applying these indices to the study and characterization of the topological properties of graphs has acquired great relevance, many topological indices have been proposed. However, extending this concept to directed graphs is a complex task since, in digraphs, each vertex has an out-degree, an in-degree, and a total degree. However, Monsalve and Rada have recently presented a generalization of VDB topological indices applied to digraphs [23]. Consequently,

there are still few works in which the properties of these topological indices have been explored [24–26].

However, understanding graph spectral properties becomes fundamental when modeling real-world systems, as these properties closely correlate with the structure of the system, evolution, and stability [10,27–30]. The spectral properties of a graph are investigated by studying the spectrum of a matrix associated with it. There are several matrix representations associated with a graph, such as the Laplacian matrix and the adjacency matrix, among others. For a simple undirected graph, the adjacency matrix $\mathbf{A}$ is defined through the matrix elements

$$A_{ij} = \begin{cases} 1 & \text{if there is an edge between vertices } i \text{ and } j, \\ 0 & \text{otherwise.} \end{cases} \tag{2}$$

The adjacency matrix of a random graph can be viewed as a random matrix, so it is possible to use tools from random matrix theory (RMT) in its analysis.

Since the pioneering studies of Wigner, the behavior of eigenvalues in random matrices has attracted considerable interest due to the observation of universal characteristics across various systems. This universality enables RMT to predict properties of emerging spectral phenomena, regardless of the systems microscopic intricacies. Notably, within RMT, it has been observed that for large matrices with independent random elements, the distribution of eigenvalues should converge to well-known Gaussian ensembles, regardless of the precise distribution of the matrix elements [31–33]. This universality extends to sparse random matrices, matrices with elements from distributions with nonzero means, and even matrices where entries are randomly chosen from a set with only two elements, as it is the case of the binary adjacency matrices of random graphs [33–37]. Therefore, exploring universality is fundamental to infer the average properties of real-world networks.

It is important to note that the adjacency matrix is not necessarily symmetric for digraphs, meaning that its eigenvalues can be complex. Similarly to the case of topological indices, this difference makes the study of spectral quantities in digraphs more significant. Even within RMT, Hermitian ensembles have received more attention than the non-Hermitian ones. Therefore, in this work, we also investigate the spectral properties of digraphs, starting with the study of the distribution of eigenvalues of digraphs in the complex plane. We explore the connection with the circle law, an extension of Wigner's semicircle law for non-Hermitian random matrices [38]. Subsequently, we investigate another spectral quantity, similar to topological indices, but related to the eigenvalues of the graphs.

In 1978 Ivan Gutman proposed the invariant $E(G)$ of a finite and undirected simple graph based on Huckel's orbital model as [39,40]

$$E(G) = \sum_{i=1}^{n} |\lambda_i|, \tag{3}$$

where λ_i are the eigenvalues of the adjacency matrix of the graph. This invariant emerges as a spectral quantity that serves as a descriptor of the properties of a graph and allows the characterization and study of the properties of specific systems. This concept was initially introduced using the eigenvalues of the adjacency matrix associated with an undirected graph.

Furthermore, other invariants defined as the sum of the absolute value of the eigenvalues associated with other graph matrices have been proposed, among them some related to the Laplacian matrix [41–43], the distance matrix [44], the incidence matrix [45], and some topological indices [46–49], etc.

Moreover, the Coulson integral is a complex integral that allows computing the invariant $E(G)$ of a graph without directly calculating its eigenvalues: Let ϕ be the characteristic polynomial of the adjacency matrix of the graph, then ϕ is the characteristic polynomial of the graph, which is defined as

$$\phi(G, x) = \det[xI - A(G)], \tag{4}$$

where I is the identity matrix of order n. The Coulson integral is defined as [50]

$$E(G) = \frac{1}{\pi} \int_{-\infty}^{\infty} \left(n - \frac{ix\phi'(G, ix)}{\phi(G, ix)} \right) dx, \tag{5}$$

where $\phi'(G, ix)$ is the derivative of $\phi(G, x)$ and n is the order of the adjacency matrix.

The invariant $E(G)$ of a graph has several applications in various fields, such as chemistry, physics, mathematics, biology, social networks, computer science, etc. [51–55]. It is mainly used as an indicator of the graph structure that determines specific properties of the system represented by the graph or to optimize specific processes. Furthermore, $E(G)$ has been used as a criterion for graph classification. Depending on its value, graphs can be categorized as hyperenergetic if $E(G) > 2(n-1)$ or nonhyperenergetic if $E(G) \leqslant 2(n-1)$; the value of $E(G)$ for a complete graph serves as a reference in this sense [56].

Thus, the interest in the study of $E(G)$ has grown significantly. The most notable results in this field focus mainly on determining upper and lower bounds for this magnitude based on various properties of the graphs, mainly of a topological nature. One of the most important bounds for $E(G)$ is the McClelland inequality, which establishes a relationship between $E(G)$ and the number of vertices and edges of the corresponding graph [57]:

$$E(G) \leqslant \sqrt{2mn}. \tag{6}$$

Remembering the fact that the eigenvalues of digraphs can be complex, the definition of the invariant $E(G)$ of Eq. (3) cannot be straightforwardly extended. Given this, several definitions of this invariant for digraphs have been proposed and studied; it will now be denoted as $E(D)$.

Therefore, this work investigates topological and spectral characteristics of directed random graphs, focusing on the Erdős-Rényi model.

II. TOPOLOGICAL AND SPECTRAL PROPERTIES OF ERDŐS-RÉNYI DIGRAPHS

A. Topological properties of Erdős-Rényi digraphs

An Erdős-Rényi (ER) digraph, denoted by $D(n, p)$, is a directed random graph with n independent vertices connected with probability p. Given two vertices u and v, p is the

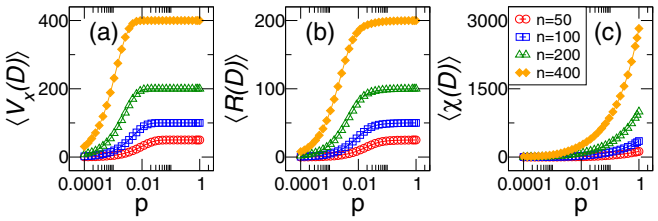

FIG. 1. (a) Average number of nonisolated vertices $\langle V_x(D)\rangle$, (b) average Randić index $\langle R(D)\rangle$, and (c) average sum-connectivity index $\langle \chi(D)\rangle$ as a function of the connection probability p of Erdős-Rényi digraphs of different sizes $n \in [50, 400]$. Each symbol was calculated by averaging over $10^6/n$ random digraphs $D(n, p)$.

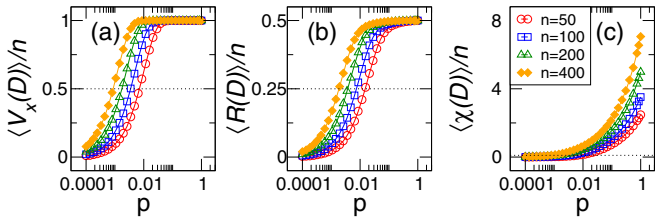

FIG. 2. (a) $\langle V_x(D)\rangle$, (b) $\langle R(D)\rangle$, and (c) $\langle \chi(D)\rangle$ normalized to n as a function of the connection probability p of Erdős-Rényi digraphs of different sizes $n \in [50, 400]$. Dotted lines in panels (a-c) correspond to 0.5, 0.25, and 0.1, respectively. Same data sets of Fig. 1.

probability that there is an arc from vertex u to vertex v, so $p \in (0, 1)$. When $p = 0$, the graph consists of n isolated vertices; when $p = 1$, it becomes a complete graph. We can obtain graphs between these two extremes by varying the value of p between 0 and 1. It is important to note that for $0 < p < 1$, a given pair of parameters (n, p) represents an infinity set of random graphs. Therefore, calculating a property for a single graph is not informative. Instead, we can obtain more relevant information by calculating a given average property over an ensemble of random graphs characterized by the same pair of parameters (n, p). Although this statistical approach is a common practice in RMT, it is not as common in graph theory; however, it has been applied recently to several random graph models [58–64].

Thus, below, we perform a numerical analysis of some topological properties of ER digraphs by the use of the number of nonisolated vertices $[V_x(D)]$ and the Randić $[R(D)]$ and the sum-connectivity $[\chi(D)]$ indices.

Following the generalization of the concept of VDB topological indices of digraphs proposed by Monsalve and Rada [23], the Randić and the sum-connectivity indices are respectively defined as

$$R(D) = \frac{1}{2}\sum_{uv\in D}\frac{1}{\sqrt{k_u^+ k_v^-}} \tag{7}$$

and

$$\chi(D) = \frac{1}{2}\sum_{uv\in D}\frac{1}{\sqrt{k_u^+ + k_v^-}}, \tag{8}$$

where uv denotes the arc connecting vertices u and v, k_u^+ denotes the out-degree of the vertex u, and k_v^- denotes the in-degree of the vertex v.

First, we compute the average values of $V_x(D)$, $R(D)$, and $\chi(D)$ for ensembles of adjacency matrices of ER digraphs characterized by different combinations of parameters (n, p). In Fig. 1, these quantities are shown for four different graph sizes as a function of the connection probability p. We can observe that the curves corresponding to each quantity follow similar shapes but are displaced in the p axis depending on the graph size. To better appreciate the shape of these curves, we normalize them to the size of the network and plot them again in Fig. 2.

In Figs. 2(a) and 2(b), it can be seen that the shape of the normalized curves of $\langle V_x(D)\rangle$ and $\langle R(D)\rangle$ are very similar. Initially, for small values of p, both are close to zero, then they increase with p until they reach their maximum values. In the case of $\langle V_x(D)\rangle/n$, the maximum value is 1, while for $\langle R(D)\rangle/n$ it is 1/2. However, Fig. 2(c) shows a different picture for the normalized curves of $\langle \chi(D)\rangle$. That is, $\langle \chi(D)\rangle/n$ is a strictly monotone increasing function and its maximum value depends on the graph size. The maximum value of $\langle \chi(D)\rangle/n$ is reached at $p = 1$ and is equal to $\sqrt{(n-1)/8}$.

Notably, in all three cases, the curves corresponding to the same quantity exhibit a similar behavior but they are shifted along the p axis for different graph sizes n. Now, our goal is to identify a scaling parameter for these quantities. To achieve this, we first need to quantify the displacement of the curves with n. Then, without loss of generality, we characterize the displacement by computing the value of p (that we label as p^*) for which $\langle V_x(D)\rangle/n$, $\langle R(D)\rangle/n$ and $\langle \chi(D)\rangle/n$ reach the value of 0.5, 0.25, and 0.1, respectively; see the dotted lines in Fig. 2.

In Fig. 3 we present p^* as a function of the graph size n and observe a linear trend of the data sets p^* versus n (in log-log scale), suggesting a power-law behavior of the form

$$p^* = \mathcal{C} n^{-\beta}. \tag{9}$$

Then, by performing numerical fittings, we determined the parameters $\mathcal{C}$ and β which are reported in Table I. There, we can clearly see that $\beta \approx 1$ in all three cases. Hence, we define the scaling parameter ξ as the ratio p/p^*,

$$\xi = \frac{p}{p^*} \propto \frac{p}{n^\beta} \propto \frac{p}{n^{-1}} = np. \tag{10}$$

Previous studies on undirected ER graphs have demonstrated that topological measures can be scaled with the average degree $\langle k\rangle$ [60–62]. Here, the average degree of ER digraphs is given by

$$\langle k\rangle = 2(n-1)p. \tag{11}$$

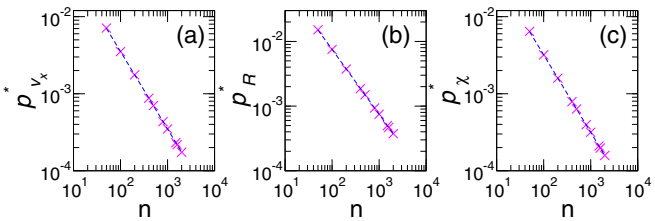

FIG. 3. p^* for (a) $\langle V_x(D)\rangle$, (b) $\langle R(D)\rangle$, and (c) $\langle \chi(D)\rangle$ as a function of the graph size n of Erdős-Rényi digraphs.

TABLE I. Values of the constants $\mathcal{C}$ and β obtained by fittings of Eq. (9) to the data in Fig. 3.

	$\langle V_x(D)\rangle$	$\langle R(D)\rangle$	$\langle \chi(D)\rangle$
$\mathcal{C}$	0.3612	0.7608	0.3271
β	1.0051	1.0026	1.005

In addition, we can observe that both $\langle k\rangle$ and ξ depend on n and p in the same functional form. Therefore, we can express ξ as a function of $\langle k\rangle$ and vice versa. Also, it is important to recall that the scaling parameter is not unique; a function of it can also serve as a scaling parameter. These observations allow us to propose the average degree $\langle k\rangle$ as the scaling parameter for the topological properties of ER digraphs. Then, in Fig. 4 we present again the curves of Fig. 2 but now plotted as a function of $\langle k\rangle$. As observed, the average degree indeed serves as the scaling parameter of these topological quantities.

Other important quantities in the study of digraphs are the number of arcs m, the number of closed walks of length two c_2, and the largest eigenvalue λ_1 (the maximum of the absolute values of the adjacency matrix eigenvalues). Our next goal is to compute these quantities and examine whether they can also be scaled with the average degree. To achieve this, we construct ensembles of ER digraphs characterized by different combinations of parameters and compute the average of the quantities above. In Fig. 5 we plot $\langle m\rangle$, $\langle c_2\rangle$, and $\langle\lambda_1\rangle$ as a function of the connection probability p. Remarkably, these quantities exhibit a behavior similar to that reported for the previously studied topological indices: Curves representing the same quantity show a similar pattern but they are shifted along the p axis for different graph sizes. This observation strongly suggests that these quantities may also be scaled with the average degree. Furthermore, Fig. 5 reveals noteworthy characteristics. Specifically, in the case of $\langle m\rangle$ and $\langle c_2\rangle$, we observe a linear trend with p on a log-log scale. Numerical calculations indicate that $\langle m\rangle$ follows the relationship $\langle m\rangle \approx n^2 p$. Similarly, for $\langle c_2\rangle$ we find that $\langle c_2\rangle \approx n^2p^2/2$. Additionally, for $p > 0.01$, we find that $\langle\lambda_1\rangle \approx np$. These approximations, where the average degree can be easily identified (i.e., $np \approx \langle k\rangle/2$), are indicated in each panel of Fig. 5 with dashed lines.

Then, in Fig. 6 we verify that the average degree indeed scales $\langle m\rangle/n$, $\langle c_2\rangle$, and $\langle\lambda_1\rangle$. Therefore we can finally write $\langle m\rangle/n \approx \langle k\rangle/2$, $\langle c_2\rangle \approx \langle k\rangle^2/8 \approx m^2/2n^2$, and $\langle\lambda_1\rangle \approx \langle k\rangle/2$ for $k > 1$; see the dashed lines in the corresponding panels of Fig. 6. These findings provide highly relevant information

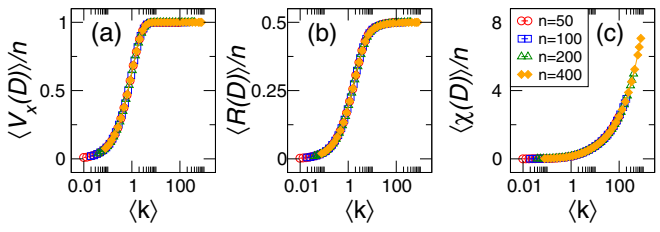

FIG. 4. (a) $\langle V_x(D)\rangle$, (b) $\langle R(D)\rangle$, and (c) $\langle\chi(D)\rangle$ normalized to n as a function of the average degree $\langle k\rangle$ of Erdős-Rényi digraphs of different sizes $n \in [50, 400]$. Same data sets of Fig. 1.

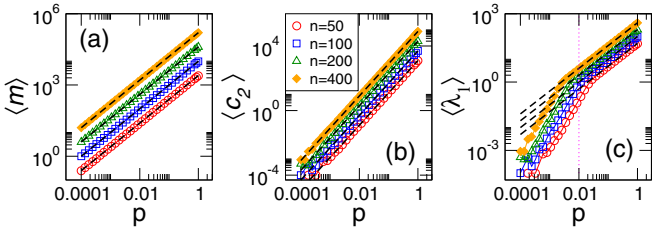

FIG. 5. (a) Average number of edges $\langle m\rangle$, (b) average number of closed walks of length 2 $\langle c_2\rangle$, and (c) average largest eigenvalue $\langle\lambda_1\rangle$ as a function of the connection probability p of Erdős-Rényi digraphs of different sizes $n \in [50, 400]$. Dashed lines in panels (a–c) correspond to $\langle m\rangle = n^2p$, $\langle c_2\rangle = n^2p^2/2$, and $\langle\lambda_1\rangle = np$, respectively. Each symbol was calculated by averaging over $10^6/n$ random digraphs.

about the relationships and scaling behavior of topological quantities, such as m and c_2, and the spectral measure λ_1, in relation to the graph parameters p, n, and $\langle k\rangle$.

In realistic networks, the largest eigenvalue λ_1 plays an important role since it is useful to determine the stability of the system [28]. We have observed that this eigenvalue scales with the average degree, which coincides with other related studies on undirected graphs of the ER type [29,30]. However, these same studies have revealed that the rest of the spectrum behaves differently. Therefore, we proceed to investigate whether the same occurs in the case of directed graphs, analyzing the rest of the spectrum and other spectral magnitudes in the next section.

B. Distribution of the adjacency matrix eigenvalues in the complex plane

The adjacency matrix of ER digraphs corresponds to a Bernoulli random matrix. This matrix is an $n \times n$ matrix with independent Bernoulli entries, where each entry has a probability p of being equal to one and a probability $(1 - p)$ of being equal to zero. When $p = 0$ the adjacency matrix of the corresponding digraph is null therefore its eigenvalues are zero, however, when $p = 1$ the adjacency matrix corresponds to a matrix with zeros on the main diagonal and all off-diagonal elements are equal to one. In this case, all the eigenvalues are real: $\lambda = -1$ with degeneracy $n - 1$ and

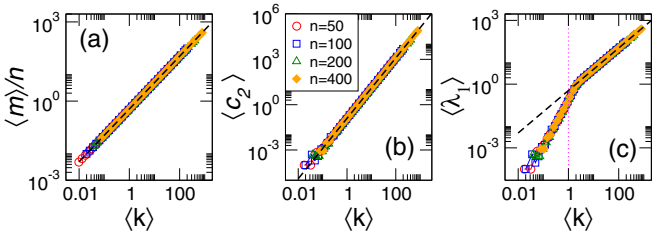

FIG. 6. (a) $\langle m\rangle/n$, (b) $\langle c_2\rangle$, and (c) $\langle\lambda_1\rangle$ as a function of the average degree $\langle k\rangle$ of Erdős-Rényi digraphs of different sizes $n \in [50, 400]$. Dashed lines in panels (a–c) correspond to $\langle m\rangle/n = \langle k\rangle/2$, $\langle c_2\rangle = \langle k\rangle^2/8 = m^2/2n^2$, and $\langle\lambda_1\rangle = \langle k\rangle/2$, respectively. Same data sets of Fig. 5.

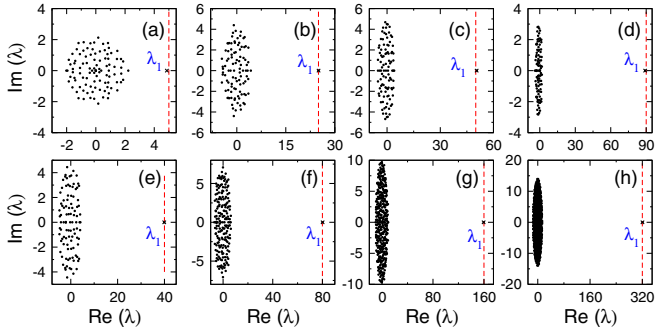

FIG. 7. Eigenvalues λ of Erdős-Rényi digraphs of several combinations of p and n. (a) $p = 0.05$ and $n = 100$, (b) $p = 0.25$ and $n = 100$, (c) $p = 0.5$ and $n = 100$, (d) $p = 0.9$ and $n = 100$, (e) $p = 0.4$ and $n = 100$, (f) $p = 0.4$ and $n = 200$, (g) $p = 0.4$ and $n = 400$, (h) $p = 0.4$ and $n = 800$. Single random graph realizations were used. The red dashed line corresponds to np. λ_1 indicates the largest eigenvalue.

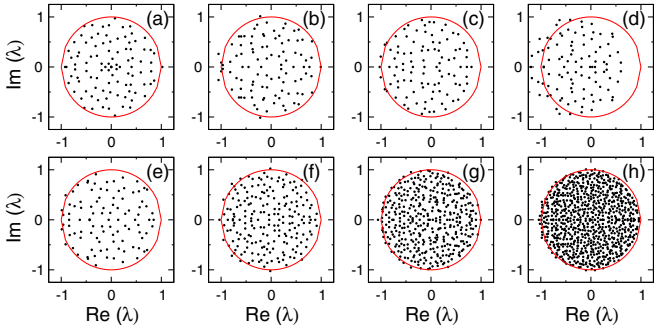

FIG. 8. Eigenvalues λ [normalized to $\sqrt{np(1-p)}$] of Erdős-Rényi digraphs of several combinations of p and n. (a) $p = 0.05$ and $n = 100$, (b) $p = 0.25$ and $n = 100$, (c) $p = 0.5$ and $n = 100$, (d) $p = 0.9$ and $n = 100$, (e) $p = 0.4$ and $n = 50$, (f) $p = 0.4$ and $n = 100$, (g) $p = 0.4$ and $n = 200$, (h) $p = 0.4$ and $n = 400$. Single random graph realizations were used.

$\lambda = n$. For intermediate values of p we observe a more interesting picture.

In Fig. 7 we plot the eigenvalues of directed ER digraphs in the complex plane for different combinations of parameters. In Figs. 7(a)–7(d), we keep the network size $n = 100$ fixed and use different values of p; in Figs. 7(e)–7(h), we fix the value of $p = 0.4$ and vary the size of the graph.

In general, we observe that the largest eigenvalue λ_1 of the digraph is separated from the bulk of the spectrum; moreover, it is real and can be well approximated by $\lambda_1 \approx np$ (red dashed lines in Fig. 7), as already anticipated in the previous section. The bulk of the spectrum is mostly contained into a circular section whose area appears to be determined by the values of the parameters n and p.

Within RMT, these observations pertain to the circular law, which is the counterpart to Wigner's semicircle law for non-Hermitian matrices [65]. The circular law states that the distribution of appropriately normalized eigenvalues from large non-Hermitian random matrices converges to the unit circle. Initially, Girko demonstrated the circular law for matrices with complex Gaussian entries [66], while Edelman later established its validity for real Gaussian matrices [67]. The circular law has attracted significant attention from researchers such as Bai, Tao, and Vu, among others [68–75]. While early investigations predominantly focused on matrices filled with random numbers possessing zero mean and unit variance, later studies have shown similar results for sparse matrices and variances different from one [76,77]. Notably, in Ref. [76], the circular law is proven for a sparse matrix $\mathbf{A}$ with zero mean and bounded variance σ^2, as well as bounded $(2+\eta)$th moment with $\eta > 0$. This law states that the eigenvalues of $\mathbf{A}/\sigma\sqrt{n}$ converge to the unit disk as $n \to \infty$. In the case of Bernoulli matrices, $\sigma^2 = p(1-p)$ and the nth moment is p. However, the mean $\mu = p$ is not zero. Nonetheless, Basak and Rudelson established in Theorem 1.7 of Ref. [78] that if $\mathbf{A}_n$ is the adjacency matrix of an ER digraph with connectivity p (i.e., a Bernoulli matrix), the distribution of the eigenvalues of $\mathbf{A}_n/\sqrt{np(1-p)}$ converges weakly to the circular law as $n \to \infty$. This is the specific case of this work and the one we decided to explore numerically below.

Subsequently, in Fig. 8, we present the bulk eigenvalues reported in Fig. 7, now normalized to $\sqrt{np(1-p)} = \sigma\sqrt{n}$. It is clear that the bulk eigenvalues are mostly contained into the unit circle in the complex plane. While an overall good correspondence is observed, it is notable that the case of $n = 100$ and $p = 0.9$ [see Fig. 8(d)] exhibits poor correspondence. Moreover, in Figs. 8(c) and 8(d), we can see that the eigenvalues are not centered around zero; this is more pronounced in Fig. 8(d).

From Fig. 8 we can conclude that $\sqrt{np(1-p)}$ may serve as a scaling parameter for spectral properties, specifically for the bulk eigenvalues. Also, since the largest eigenvalue λ_1 is the only eigenvalue located far from the bulk of the spectrum, we expect the second-largest eigenvalue, λ_2, to be well approximated by $\sqrt{np(1-p)}$ which determines the radius of convergence of the bulk eigenvalues.

So, we now explore some properties of the second-largest eigenvalue λ_2. For this, we fix the value of $\sqrt{np(1-p)}$ and plot the distribution of λ_2 for different combinations of n and p, as shown in Fig. 9. Taking Fig. 8 as a reference, we choose (a) $\sqrt{np(1-p)} \approx 2.18$, (b) $\sqrt{np(1-p)} \approx 4.33$, (c) $\sqrt{np(1-p)} = 5$, and (d) $\sqrt{np(1-p)} = 3$, which correspond to the digraphs used in Figs. 8(a)–8(d), respectively. In black dashed lines, we indicate the values of $\sqrt{np(1-p)}$.

We can notice that as the size of the graph increases, the peak of the distribution of the second-largest eigenvalue approaches the value of $\sqrt{np(1-p)}$; as expected from Ref. [78].

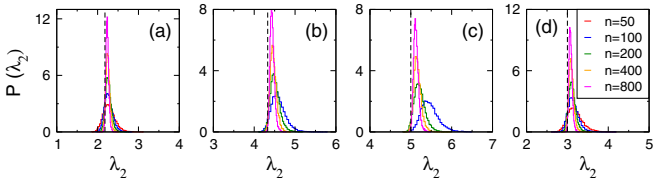

FIG. 9. Distribution of the second-largest eigenvalue λ_2 of Erdős-Rényi graphs for different parameter combinations such that the variance is fixed to (a) $\sqrt{np(1-p)} = 2.18$, (b) $\sqrt{np(1-p)} = 4.33$, (c) $\sqrt{np(1-p)} = 5$, and (d) $\sqrt{np(1-p)} = 3$. Black dashed lines corresponds to $\sqrt{np(1-p)}$.

However, we notice that for $\sqrt{np(1-p)} = 5$ a large deviation is observed, especially for the case $n = 100$ which corresponds to $p = 0.5$. Despite of this, in general, $\sqrt{np(1-p)}$ can be used as the scaling parameter for the bulk of eigenvalues.

III. THE INVARIANT $E(D)$ OF ERDŐS-RÉNYI DIGRAPHS

A. Short review of the invariant $E(D)$

As mentioned in the Introduction, the definition of the invariant $E(G)$ proposed by Gutman [see Eq. (3)] cannot be directly applied to digraphs since, in this case, the eigenvalues can be complex. In the case of digraphs, the invariant is denoted as $E(D)$. However, by examining Eq. (3), a straightforward generalization can be done by replacing the absolute value of the real eigenvalues with the module of the complex eigenvalues of the adjacency matrix of a digraph, here denoted as Z_k. In fact, this definition,

$$\mathcal{S}(D) = \sum_{k=1}^{n} |Z_k|, \tag{12}$$

has been reported in Ref. [79]. Interestingly, this definition is not the most widely studied. Instead of opting for this direct generalization, other definitions have received more attention.

In Ref. [80], Peña and Rada, motivated by Coulson's formula, generalized the concept of $E(D)$ of a digraph as

$$e(D) = \sum_{k=1}^{n} |\operatorname{Re}(Z_k)|. \tag{13}$$

$e(D)$ has been extensively studied; see for example Refs. [81–85]. Also, this definition has been extended to other graph invariants [86,87]. Bounds have also been established for $e(D)$. For example, in Ref. [85] Rada generalized McClelland's inequality for directed graphs with n vertices, m edges, and c_2 closed walks of length 2 as

$$e(D) \leqslant \sqrt{\frac{1}{2}n(m + c_2)}. \tag{14}$$

Also, a lower bound for $e(D)$ was established [81,82]:

$$e(D) \geqslant \sqrt{2c_2}. \tag{15}$$

It is important to note that the definition of Peña and Rada, although it satisfies the Coulson integral, does not consider the imaginary part of the eigenvalues.

Another definition that does consider the imaginary part of the eigenvalues was proposed by Khan, Farooq, and Rada in Ref. [88]. This is the iota invariant and is defined as

$$E_\iota(D) = \sum_{k=1}^{n} |\operatorname{Im}(Z_k)|. \tag{16}$$

$E_\iota(D)$ can be defined from the Coulson integral formula using the characteristic polynomial of the complex adjacency matrix $\mathbf{A}_c$. Which is defined as

$$\mathbf{A}_{c_{uv}} = \begin{cases} -\iota & \text{if } u \to v, \\ 0 & \text{otherwise.} \end{cases} \tag{17}$$

$E_\iota(D)$ has been extensively studied in digraphs with specific characteristics such as bicyclic, tricyclic, and signed digraphs [89–93].

More recently, Khan proposed another definition incorporating both real and imaginary parts of the adjacency matrix eigenvalues. This invariant is defined as [94,95]

$$E_p(D) = \sum_{k=1}^{n} |\operatorname{Re}(Z_k)\operatorname{Im}(Z_k)|. \tag{18}$$

To represent $E_p(D)$ in an integral way with Coulson's formula, it is necessary to use the characteristic polynomial of the squared adjacency matrix $\mathbf{A}^2$ instead of the characteristic polynomial of $\mathbf{A}$.

Moreover, Nikiforov [96] proposed a similar invariant but using the corresponding singular values. The singular values of a matrix are a set of nonnegative elements that are calculated from a matrix $\mathbf{A} \in \mathcal{R}^{m\times n}$. They are defined as the square root of the eigenvalues of the $\mathbf{A}^T\mathbf{A} \in \mathcal{R}^{n\times n}$ matrix. Given the singular values of a matrix $\mathbf{A}$, σ_k, the Nikiforov invariant is defined as

$$\mathcal{N}(\mathbf{A}) = \sum_{k=1}^{n} \sigma_k. \tag{19}$$

This concept has been widely studied for different types of matrices, such as nonsquare matrices [97] and for digraphs [98,99]. Its importance lies in the fact that it can be computed for any matrix and, in the case of a square symmetric matrix, it reproduces Eq. (3). For the Nikiforov invariant, some bounds have been reported in terms of the properties of the matrix. Particularly, an upper bound for $\mathcal{N}(D)$ has been reported as [81,97]

$$\mathcal{N}(D) \leqslant \frac{m}{n} + \sqrt{(n-1)\left(m - \frac{m^2}{n^2}\right)}, \tag{20}$$

while Agudelo and Rada proposed the lower bound [98]

$$\mathcal{N}(D) \geqslant \sqrt{m}. \tag{21}$$

Another definition of invariant reported in the literature is the Hermitian invariant [100–102]. In contrast to the previous definitions, this invariant is not directly linked to the adjacency matrix of the digraph. To calculate this invariant, it is necessary to construct the Hermitian adjacency matrix, denoted as $\mathbf{H}$, which is defined as follows:

$$H_{uv} = \begin{cases} 1 & \text{if } u \leftrightarrow v, \\ -\iota & \text{if } u \to v, \\ \iota & \text{if } v \to u, \\ 0 & \text{otherwise.} \end{cases} \tag{22}$$

Since $\mathbf{H}$ is a Hermitian matrix by construction, its eigenvalues are real. Then, the Hermitian invariant, denoted as $E_H(G)$, can be computed using Eq. (3) with the eigenvalues of $\mathbf{H}$. Bounds have also been established for $E_H(G)$. Considering q as the determinant of $\mathbf{H}$ and Δ the maximum degree of the graph, the following bounds were derived [100]:

$$\sqrt{2m + n(n-1)q^{2/n}} \leqslant E_H(G) \leqslant n\sqrt{\Delta}. \tag{23}$$

Additionally, when considering solely the number of arcs, an alternative bound for the Hermitian invariant is expressed as [100]

$$2\sqrt{m} \leqslant E_H(G) \leqslant 2m. \tag{24}$$

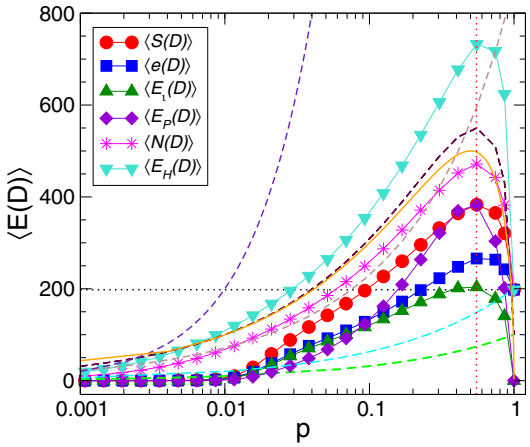

FIG. 10. Average invariants $E(D)$ as a function of the connection probability p of Erdős-Rényi digraphs of size $n = 100$. The dashed lines indicate the limits defined by Eqs. (14) (brown color), (20) (maroon color), (21) (green color), and the upper and lower bounds given by Eq. (25) (violet and cyan, respectively). The black dotted line indicates the hyperenergetic limit. The vertical red-dotted line is $p = \frac{1}{2}(1 + \frac{1}{\sqrt{n}})$ with $n = 100$. The yellow solid line corresponds to $\sqrt{np(1-p)}$. Each symbol was calculated by averaging over $10^6/n$ random digraphs.

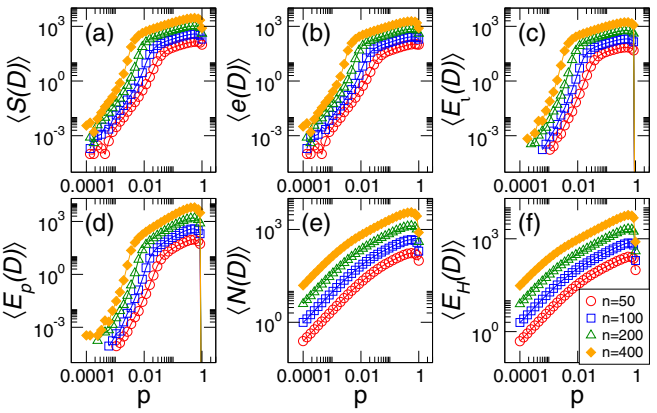

FIG. 11. Average invariants (a) $\langle \mathcal{S}(D) \rangle$, (b) $\langle e(D) \rangle$, (c) $\langle E_\iota(D) \rangle$, (d) $\langle E_p(D) \rangle$, (e) $\langle \mathcal{N}(D) \rangle$, and (f) $\langle E_H(D) \rangle$ as a function of the connection probability p of Erdős-Rényi digraphs of sizes $n \in [50, 400]$. Each symbol was calculated by averaging over $10^6/n$ random digraphs.

Particularly for ER digraphs, considering the relationships of m, n, and p found in the previous section, this bound can be expressed as

$$2n\sqrt{p} \leqslant E_H(G) \leqslant 2n^2 p. \tag{25}$$

Although all these invariants have been extensively studied to determine minimum and maximum bounds and have also been computed for specific graphs, no numerical study has yet been performed to compare them. To fill this gap, we have undertaken the task of numerically and statistically evaluating these invariants for ensembles of ER random digraphs.

B. Invariant $E(D)$ of ER digraphs

Here we compute the invariants $\mathcal{S}(D)$, $e(D)$, $E_\iota(D)$, $E_p(D)$, $\mathcal{N}(D)$, and $E_H(D)$ for ensembles of ER digraphs characterized by the parameter pair (n, p).

Then, in Fig. 10, we plot the average invariants of ER digraphs of size $n = 100$ as a function of the connection probability p. In Fig. 10 we also indicate the bounds given by Eqs. (14), (20), (21), and (25), and the hyperenergetic limit $2n - 2$.

From Fig. 10, we can see that all invariants exhibit a similar pattern as a function of p: As p increases, the invariants increase until reaching a maximum value at p close to 1; then, its decrease displaying a bell-like shape that is better observed in a semilogarithmic scale. However, the maximum values for different invariants are different. We numerically computed the maximum values reached by the different invariants for ensembles of digraphs of different sizes (not shown here). We found that all invariants reach their maximum at $p \approx 0.5$. Moreover, we can see in Fig. 10 that the curve corresponding to Eq. (20) also reaches its maximum at $p \approx 0.5$, in agreement with all the numerically computed invariants. Then, to get an estimation of the value of p producing the invariant maxima we rewrite Eq. (20) in terms of n and p using $m \approx n^2 p$, then we see that

$$\begin{aligned} \mathcal{N}(D) &\leqslant np + \sqrt{(n-1)(n^2 p - n^2 p^2)} \\ &= np + n\sqrt{(n-1)p(1-p)}. \end{aligned} \tag{26}$$

So we find that the maximum of Eq. (26) occurs at $p = \frac{1}{2}(1 + \frac{1}{\sqrt{n}})$, which is consistent with the numerical observation. From Eq. (26) we also observe that we can relate the Nikiforov invariant to $\sqrt{np(1-p)}$, as

$$\mathcal{N}(D) \leqslant np + n\sqrt{np(1-p)}. \tag{27}$$

Given that $\sqrt{np(1-p)} > p$, in general, in Fig. 10, we include $\sqrt{np(1-p)}$ (see the yellow line) and observe that this quantity has the shape of the invariant curves and can also be used as an upper bound for most of the invariants (except for the Hermitian).

We recall that in Fig. 10 we used ER digraphs of size $n = 100$ so, to see the effect of the graph size on the average invariants; in Fig. 11, we plot them as a function of p for different values of n. From this figure, we can observe that the curves for a given invariant definition exhibit a similar functional dependence of p, but they are shifted on both axes for increasing n. This effect of n on the invariants is equivalent to that observed in the previous Section for the topological and spectral properties of ER digraphs, see Figs. 1 and 5. Considering that $\sqrt{np(p-1)}$ fixes the distribution of the bulk of the eigenvalues, we now plot the invariants (normalized to n) as a function of $\sqrt{np(p-1)}$. Indeed, we observe that $\sqrt{np(p-1)}$ works well as the scaling parameter of the normalized invariants, mainly above the percolation threshold $\langle k \rangle > 1$.

In the panels of Fig. 12, we also include $\sqrt{np(p-1)}$ for $n = 400$ (red dashed lines) and observe that it effectively works as a bound for the invariants, except for the Hermitian. Moreover, remarkably, $\sqrt{np(p-1)}$ perfectly scales the normalized Nikiforov invariant as well as the normalized Hermitian invariant over the entire range of connection

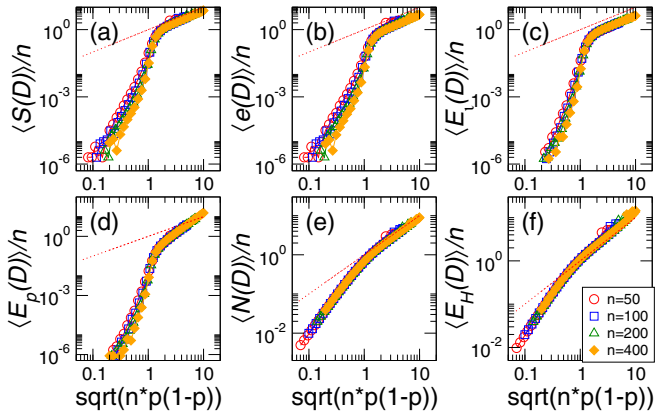

FIG. 12. (a) $\langle \mathcal{S}(D)\rangle$, (b) $\langle e(D)\rangle$, (c) $\langle E_\iota(D)\rangle$, (d) $\langle E_p(D)\rangle$, (e) $\langle \mathcal{N}(D)\rangle$, and (f) $\langle E_H(D)\rangle$ normalized to n as a function of $\sqrt{np(1-p)}$ of Erdős-Rényi digraphs of sizes $n \in [50, 400]$. Same data sets of Fig. 11. The red dashed line corresponds to $\sqrt{np(1-p)}$ for $n = 400$.

probabilities, see Figs. 12(e) and 12(f). We can notice that the worst scaling is given for the invariants $\mathcal{S}(D)$ and $e(D)$, which is attributable to the contribution of the largest eigenvalue which is quite far from the bulk eigenvalues and it scales with the average degree: $\lambda_1 \approx \langle k\rangle/2$.

In addition, in Fig. 12 we can see that certain invariants pairs depend on $\sqrt{np(p-1)}$ in a very similar way and, consequently, they should be strongly correlated. Specifically, we observe strong similarities between $\mathcal{S}(D)$ and $e(D)$, see Figs. 12(a) and 12(b), and between $\mathcal{N}(D)$ and $E_H(D)$, see Figs. 12(e) and 12(f). So, in Fig. 13, we present scatter plots of these pairs of invariants and report the corresponding Pearson correlation coefficients. Moreover, the strong correlations reported in Fig. 13 allowed us to state the following relations:

$$\sqrt{2}\, e(D) \approx \mathcal{S}(D), \tag{28}$$

$$E_H(D) \approx \tfrac{8}{5}\, \mathcal{N}(D), \tag{29}$$

see the black-dashed lines Fig. 13.

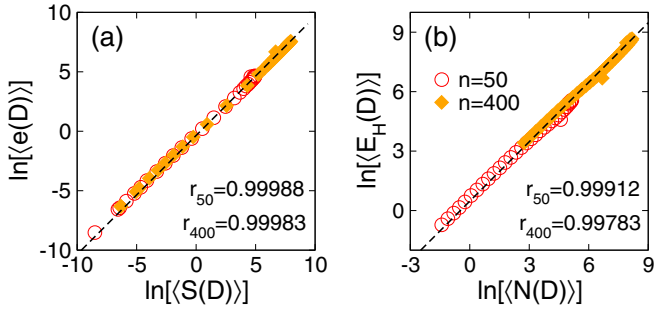

FIG. 13. Scatter plots of (a) $\langle \mathcal{S}(D)\rangle$ vs $\langle e(D)\rangle$ and (b) $\langle \mathcal{N}(D)\rangle$ vs $\langle E_H(D)\rangle$. Data corresponds to $n = 50$ and 400. The Pearson correlation coefficients r are reported in the corresponding panels. The black-dashed lines are fittings of the form $y = \mathcal{C}x$, with (a) $\mathcal{C} = 1/\sqrt{2}$ and (b) $\mathcal{C} = 8/5$.

IV. CONCLUSIONS AND DISCUSSION

This study aims to contribute to the understanding of topological and spectral properties of random digraphs. Specifically, we studied some topological and spectral properties of Erdős-Rényi (ER) digraphs $D(n, p)$.

Initially, we focused on the statistical analysis of topological properties by computing the average number of nonisolated vertices $\langle V_x(D)\rangle$, the average Randić index $\langle R(D)\rangle$ and the average sum-connectivity index $\langle \chi(D)\rangle$. By means of a scaling analysis, we found that the total average degree $\langle k\rangle$ works well as scaling parameter of $\langle V_x(D)\rangle$, $\langle R(D)\rangle$ and $\langle \chi(D)\rangle$ but also for the average number of arcs $\langle m(D)\rangle$, the average largest eigenvalue $\langle \lambda_1(D)\rangle$ and the average closed walks of length 2 $\langle c_2(D)\rangle$. Moreover, we were able to infer the following relations: $\langle m(D)\rangle/n \approx \langle k\rangle/2$, $\langle c_2(D)\rangle \approx \langle k\rangle^2/8$, and $\langle \lambda_1(D)\rangle \approx \langle k\rangle/2$ for $\langle k\rangle > 1$.

Concerning spectral properties, we first explore the distribution of the eigenvalues in the complex plane and observe that the bulk eigenvalues mostly fall within the circle of radius $\sqrt{np(p-1)}$. We also note that this quantity fixes the statistical properties of the second-largest eigenvalue. Subsequently, we computed six different graph invariants for ensembles of ER digraphs $D(n, p)$: $\mathcal{S}(D)$, $e(D)$, $E_\iota(D)$, $E_p(D)$, $\mathcal{N}(D)$, and $E_H(D)$. Then, we showed that $\sqrt{np(1-p)}$ scales well all the normalized averaged invariants, mainly scales $\langle \mathcal{N}(D)\rangle/n$ and $\langle E_H(D)\rangle/n$ over the entire range of connection probabilities. We also observe that $\sqrt{np(p-1)}$ is an upper limit for most invariants.

Then, we reformulated a set of bounds previously reported in the literature for these quantities as a function (n, p). So, by identifying strong correlations between $\mathcal{S}(D)$ and $e(D)$, and between $\mathcal{N}(D)$ and $E_H(D)$ we phenomenologically stated linear relations between invariants; see Eqs. (28) and (29).

It is important to stress that Eqs. (28) and (29) can be used to extend previously known bounds. That is, from Eqs. (14) and (15) and (28) we get

$$2\sqrt{c_2} \leqslant S(D) \leqslant \sqrt{n(m + c_2)},$$

by combining Eqs. (20), (21), and (29) we can write

$$\frac{8}{5}\sqrt{m} \leqslant E_H(D) \leqslant \frac{8}{5}\left[\frac{m}{n} + \sqrt{(n-1)\left(m - \frac{m^2}{n^2}\right)}\right],$$

while from Eqs. (24) and (29) we obtain

$$\tfrac{5}{4}\sqrt{m} \leqslant \mathcal{N}(D) \leqslant \tfrac{5}{4}m,$$

which in the particular case of ER digraphs, read as

$$\sqrt{2}np \leqslant S(D) \leqslant n\sqrt{np\left(1 + \frac{p}{2}\right)}, \tag{30}$$

$$\frac{8}{5}n\sqrt{p} \leqslant E_H(D) \leqslant \frac{8}{5}n[p + \sqrt{(n-1)p(1-p)}], \tag{31}$$

and

$$\tfrac{5}{4}n\sqrt{p} \leqslant \mathcal{N}(D) \leqslant \tfrac{5}{4}n^2 p, \tag{32}$$

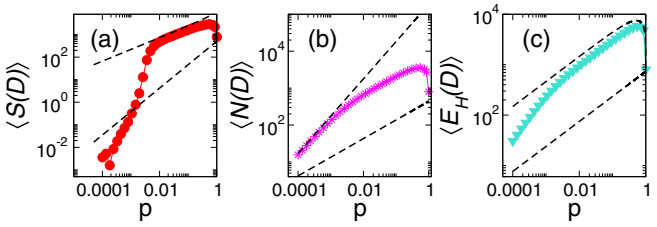

FIG. 14. (a) $\langle \mathcal{S}(D) \rangle$, (b) $\langle \mathcal{N}(D) \rangle$, and (c) $\langle E_H(D) \rangle$ as a function of the connection probability p of Erdős-Rényi digraphs of size $n = 400$. The dashed lines in panels (a), (b), and (c) indicate the limits given by Eqs. (30), (31), and (32), respectively.

respectively. Finally, in Fig. 14, we validate Eqs. (30) and (32) on ER digraphs of size $n = 400$. We just note that the lower bound in Eq. (30) fails to bound $\langle \mathcal{S}(D) \rangle$, see Fig. 14(a); however, this also happens in the original Eq. (15).

Finally, it is interesting to suggest as future work the continuation of the study of properties that imply dynamics within these digraphs, especially it would be interesting to explore the case of random walks.

ACKNOWLEDGMENTS

J.A.M.-B. thanks support from CONAHCyT (Grant No. 286633), CONAHCyT-Fronteras (Grant No. 425854), and VIEP-BUAP (Grant No. 100405811-VIEP2024), Mexico. C.T.M.-M. thanks CONAHCYT for support (CVU No. 784756).

[1] A. L. Barabási, *Network Science* (Cambridge University Press, Cambridge, UK, 2016).
[2] M. Newman, *Networks: An Introduction* (Oxford University Press, Oxford, UK, 2010).
[3] R. Albert and A. L. Barabási, Statistical mechanics of complex networks, Rev. Mod. Phys. **74**, 47 (2002).
[4] M. Gosak, R. Markovič, J. Dolenšek, M. Slak Rupnik, M. Marhl, A. Stožer, and M. Perc, Network science of biological systems at different scales: A review, Phys. Life Rev. **24**, 118 (2018).
[5] S. P. Borgatti and D. S. Halgin, Analyzing affiliation networks, Sage Handb. Soc. Netw. Anal. **1**, 417 (2011).
[6] M. E. Newman, The structure and function of complex networks, SIAM Rev. **45**, 167 (2003).
[7] V. Latora and M. Marchiori, Efficient behavior of small-world networks, Phys. Rev. Lett. **87**, 198701 (2001).
[8] C. F. Negre, U. N. Morzan, H. P. Hendrickson, R. Pal, G. P. Lisi, J. P. Loria, I. Rivalta, J. Ho, and V. S. Batista, Eigenvector centrality for characterization of protein allosteric pathways, Proc. Natl. Acad. Sci. USA **115**, E12201 (2018).
[9] T. Martin, X. Zhang, and M. E. J. Newman, Localization and centrality in networks, Phys. Rev. E **90**, 052808 (2014).
[10] S. Allesina, A. Bodini, and C. Bondavalli, Ecological subsystems via graph theory: The role of strongly connected components, Oikos **110**, 164 (2005).
[11] S. Levine, Several measures of trophic structure applicable to complex food webs, J. Theor. Biol. **83**, 195 (1980).
[12] A. C. Zorach and R. E. Ulanowicz, Quantifying the complexity of flow networks: How many roles are there? Complexity **8**, 68 (2003).
[13] O. Sporns and J. D. Zwi, The small world of the cerebral cortex, Neuroinformatics **2**, 145 (2004).
[14] O. Sporns, D. R. Chialvo, M. Kaiser, and C. C. Hilgetag, Organization, development and function of complex brain networks, Trends Cogn. Sci. **8**, 418 (2004).
[15] M. Rubinov and O. Sporns, Complex network measures of brain connectivity: Uses and interpretations, NeuroImage **52**, 1059 (2010).
[16] A. L. Barabási, N. Gulbahce, and J. Loscalzo, Network medicine: A network-based approach to human disease, Nat. Rev. Genet. **12**, 56 (2011).
[17] A. van der Schaft, S. Rao, and B. Jayawardhana, On the mathematical structure of balanced chemical reaction networks governed by mass action kinetics, SIAM J. Appl. Math. **73**, 953 (2013).
[18] M. Pérez Millán, A. Dickenstein, A. Shiu, and C. Conradi, Chemical reaction systems with toric steady states, Bull. Math. Biol. **74**, 1027 (2012).
[19] J.N.M. de Souza, J. L. De Medeiros, A. L. H. Costa, and G. C. Nunes, Modeling, simulation and optimization of continuous gas lift systems for deepwater offshore petroleum production, J. Pet. Sci. Eng. **72**, 277 (2010).
[20] H. Kamberaj, Heat flow random walks in biomolecular systems using symbolic transfer entropy and graph theory, J. Mol. Graphics Model. **104**, 107838 (2021).
[21] D. Acemoglu, A. Ozdaglar, and A. Tahbaz-Salehi, Systemic risk and stability in financial networks, Am. Econ. Rev. **105**, 564 (2015).
[22] I. Gutman, Degree-based topological indices, Croat. Chem. Acta **86**, 351 (2013).
[23] J. Monsalve and J. Rada, Vertex-degree based topological indices of digraphs, Discret. Appl. Math. **295**, 13 (2021).
[24] J. Monsalve and J. Rada, Sharp upper and lower bounds of VDB topological indices of digraphs, Symmetry **13**, 1903 (2021).
[25] R. Cruz, J. Monsalve, and J. Rada, Randic energy of digraphs, Heliyon **8**, e11874 (2022).
[26] G. Arizmendi and O. Arizmendi, Energy and Randić index of directed graphs, Linear Multilinear Alg. **71**, 2696 (2022).
[27] S. Allesina and S. Tang, The stability-complexity relationship at age 40: A random matrix perspective, Popul. Ecol. **57**, 63 (2015).
[28] S. Allesina and S. Tang, Stability criteria for complex ecosystems, Nature (London) **483**, 205 (2012).
[29] I. J. Farkas, I. Derényi, A. L. Barabási, and T. Vicsek, Spectra of real-world graphs: Beyond the semicircle law, Phys. Rev. E **64**, 026704 (2001).
[30] S. Jalan, G. Zhu, and B. Li, Spectral properties of directed random networks with modular structure, Phys. Rev. E **84**, 046107 (2011)
[31] M. L. Mehta, *Random Matrices*, 3rd ed (Academic Press, Amsterdam, 2004).

[32] L. Erdős and H. T. Yau, A comment on the Wigner-Dyson-Mehta bulk universality conjecture for Wigner matrices, Electron. J. Probab. **17**, 1 (2012).

[33] T. Tao and V. Vu, Random matrices: Universality of the local eigenvalue statistics, Acta Math. **206**, 127 (2011).

[34] L. Erdős, H. T. Yau, and J. Yin, Universality for generalized Wigner matrices with Bernoulli distribution, J. Comb. **2**, 15 (2011).

[35] L. Erdős, A. Knowles, H. T. Yau, and J. Yin, Spectral statistics of Erdos-Renyi graphs: I. Local semicircle law, Ann. Probab. **41**, 2279 (2013).

[36] L. Erdős, A. Knowles, H. T. Yau, and J. Yin, Spectral statistics of Erdos-Renyi graphs: II. Eigenvalue spacing and the extreme eigenvalues, Commun. Math. Phys. **314**, 587 (2012).

[37] C. H. Joyner and U. Smilansky, Spectral statistics of Bernoulli matrix ensembles—A random walk approach (I), J. Phys. A: Math. Theor. **48**, 255101 (2015).

[38] M. L. Mehta, *Random Matrices and the Statistical Theory of Energy Levels* (Academic Press, San Diego, CA, 1967).

[39] I. Gutman, The energy of a graph, Ber. Math.-Statist. Sekt. For. Graz **103**, 1 (1978).

[40] I. Gutman, The energy of a graph: Old and new results, *Algebraic Combinatorics and Applications* (Springer, Berlin, 2001).

[41] I. Gutman and B. Zhou, Laplacian energy of a graph, Linear Alg. Appl. **414**, 29 (2006).

[42] J. Liu and B. Liu, A Laplacian energy like invariant of a graph, MATCH Commun. Math. Comput. Chem. **59**, 355 (2008).

[43] W. So, M. Robbiano, N. M. M. de Abreu, and I. Gutman, Applications of a theorem by Ky Fan in the theory of graph energy, Linear Alg. Appl. **432**, 2163 (2010).

[44] G. Indulal, I. Gutman, and A. Vijayakumar, On distance energy of graphs, MATCH Commun. Math. Comput. Chem. **60**, 461 (2008).

[45] M. R. Jooyandeh, D. Kiani, and M. Mirzakhah, Incidence energy of a graph, MATCH Commun. Math. Comput. Chem. **62**, 561 (2009).

[46] C. Adiga, R. Balakrishnan, and W. So, The skew energy of a digraph, Lin. Alg. Appl. **432**, 1825 (2010).

[47] K. J. Gowtham and S. N. Narasimha, On Sombor energy of graphs, Nanosystems: Phys. Chem. Math. **12**, 411 (2021).

[48] Ş B. Bozkurt, A. D. Güngör, I. Gutman, and A. S. Çevik, Randić matrix and Randić energy, MATCH Commun. Math. Comput. Chem. **64**, 239 (2010).

[49] W. H. Haemers, Seidel switching and graph energy, MATCH Commun. Math. Comput. Chem. **68**, 653 (2012).

[50] C. A. Coulson, On the calculation of the energy in unsaturated hydrocarbon molecules, Math. Proc. Camb. Phil. Soc. **36**, 201 (1940).

[51] M. Dehmer, L. A. J. Mueller, and F. Emmert-Streib, Quantitative network measures as biomarkers for classifying prostate cancer disease states: A systems approach to diagnostic biomarkers, PLoS One **8**, e77602 (2013).

[52] M. Dehmer, M. Grabner, and B. Furtula, Structural discrimination of networks by using distance, degree, and eigenvalue-based measures, PLoS One **7**, e38564 (2012).

[53] D. Xu, H. Xu, Y. Zhang, W. Chen, and R. Gao, Protein-protein interactions prediction based on graph energy and protein sequence information, Molecules **25**, 1841 (2020).

[54] A. Shojaie and N. Sedaghat, *How different are estimated genetic networks of cancer subtypes? Big and Complex Data Analysis: Methodologies and Applications* (Springer, Berlin, 2017).

[55] S. S. Kamath and S. Mahadevi, Graph energy-based centrality measure to identify influential nodes in social networks, in *Proceedings of the IEEE 5th International Conference for Convergence in Technology (I2CT)*, (IEEE, Piscataway, NJ, 2019), pp. 1–6.

[56] R. Balakrishnan, The energy of a graph, Linear Alg. Appl. **387**, 287 (2004).

[57] B. J. McClelland, Properties of the latent roots of a matrix: The estimation of π-electron energies, J. Chem. Phys. **54**, 640 (1971).

[58] R. Aguilar-Sanchez, I. F. Herrera-Gonzalez, J. A. Mendez-Bermudez, and J. M. Sigarreta, Computational properties of general indices on random networks, Symmetry **12**, 1341 (2020).

[59] R. Aguilar-Sanchez, J. A. Mendez-Bermudez, F. A. Rodrigues, and J. M. Sigarreta, Topological versus spectral properties of random geometric graphs, Phys. Rev. E **102**, 042306 (2020).

[60] C.T. Martínez-Martínez, J. A. Mendez-Bermudez, J. M. Rodriguez, and J. M. Sigarreta-Almira, Computational and analytical studies of the Randić index in Erdøs-Rényi models, Appl. Math. Comput. **377**, 125137 (2020).

[61] C. T. Martínez-Martínez, J. A. Méndez-Bermúdez, José M Rodríguez, and José M Sigarreta, Computational and analytical studies of the Harmonic index on Erdös-Rényi models, Math. Comput. Chem. **85**, 395 (2021)

[62] J. A. Mendez-Bermudez, A. Alcazar-Lopez, A. J. Martinez-Mendoza, F. A. Rodrigues, and T. K. DM. Peron, Universality in the spectral and eigenfunction properties of random networks, Phys. Rev. E **91**, 032122 (2015).

[63] T. Peron, F. de Resende Bruno Messias, F. A. Rodrigues, L. D. F. Costa, and J. A. Méndez-Bermúdez, Spacing ratio characterization of the spectra of directed random networks, Phys. Rev. E **102**, 062305 (2020).

[64] K. Peralta-Martinez and J. A. Méndez-Bermúdez, Directed random geometric graphs: Structural and spectral properties, J. Phys. Complex. **4**, 015002 (2023).

[65] J. Ginibre, Statistical ensembles of complex, quaternion, and real matrices, J. Math. Phys. **6**, 440 (1965).

[66] V. L. Girko, Circular law, Theory Probab. Appl. **29**, 694 (1985).

[67] A. Edelman, The probability that a random real Gaussian matrix has k real eigenvalues, related distributions, and the circular law, J. Multivariate Anal. **60**, 203 (1997).

[68] Z. D. Bai, Circular law, Ann. Probab. **25**, 494 (1997).

[69] Z. D. Bai and J. W. Silverstein, *Spectral Analysis of Large Dimensional Random Matrices*, Mathematics Monograph Series 2 (Science Press, Beijing, 2006).

[70] V. L. Girko, The circular law: Ten years later, Random Oper. Stoch. Eq. **2**, 235 (1994).

[71] V. L. Girko, The strong circular law. Twenty years later. I, Random Oper. Stoch. Eq. **12**, 49 (2004).

[72] V. L. Girko, The strong circular law. Twenty years later. II, Random Oper. Stoch. Eq. **12**, 255 (2004).

[73] V. L. Girko, The circular law. Twenty years later. III, Random Oper. Stoch. Eq. **13**, 53 (2005).

[74] T. Tao and V. Vu, Random matrices: Universality of ESDs and the circular law, Ann. Probab. **38**, 2023 (2010).
[75] C. Bordenave and D. Chafaï, Around the circular law, Probab. Surv. **9**, 1 (2012).
[76] T. Tao and V. Vu, Random matrices: The circular law, Commun. Contemp. Math. **10**, 261 (2008).
[77] P. M. Wood, Universality and the circular law for sparse random matrices, Ann. Appl. Probab. **22**, 1266 (2012).
[78] A. Basak and M. Rudelson, The circular law for sparse non-Hermitian matrices, Ann. Probab. **47**, 2359 (2019).
[79] M. Mateljević, V. Božin, and I. Gutman, Energy of a polynomial and the Coulson integral formula, J. Math. Chem. **48**, 1062 (2010).
[80] I. PeÑa and J. Rada, Energy of digraphs, Linear Multilinear Alg. **56**, 565 (2008).
[81] R. A. Brualdi, Spectra of digraph, Linear Alg. Appl. **432**, 2181 (2010).
[82] J. Rada, Lower bounds for the energy of digraphs, Linear Alg. Appl. **432**, 2174 (2010).
[83] J. Rada, Bounds for the energy of normal digrahs, Linear Multilinear Alg. **60**, 323 (2012).
[84] S. Pirzada, M. A. Bhat, I. Gutman, and J. Rada, On the energy of digraphs, Bull. IMVI **3**, 69 (2013).
[85] J. Rada, The McClelland inequality for the energy of digraphs, Linear Alg. Appl. **430**, 800 (2009).
[86] I. Gutman, Comparative studies of graph energies. Bulletin (Académie serbe des sciences et des arts. Classe des sciences mathématiques et naturelles, Sciences Mathématiques) **37**, 1 (2012).
[87] X. Li, Y. Shi, and I. Gutman, *Graph Energy* (Springer, New York, NY, 2012).
[88] M. Khan, R. Farooq, and J. Rada, Complex adjacency matrix and energy of digraphs, Linear Multilinear Alg. **65**, 2170 (2017).
[89] R. Farooq, M. Khan, and F. Ahmad, Extremal iota energy of bicyclic digraphs, Appl. Math. Comput. **303**, 24 (2017).
[90] X. Yang and L. Wang, On the ordering of bicyclic digraphs with respect to energy and iota energy, Appl. Math. Comput. **339**, 768 (2018).
[91] R. Farooq, M. Khan, and S. Chand, On iota energy of signed digraphs, Linear Multilinear Alg. **67**, 705 (2019).
[92] R. Farooq, S. Chand, and M. Khan, Iota energy of bicyclic signed digraphs, Asian-Eur. J. Math. **12**, 1950078 (2019).
[93] J. Fareeha and K. Khan, Extremal Iota energy of a subclass of tricyclic digraphs and sidigraphs, Matriks Sains Matematik **2**, 40 (2018).
[94] M. Khan, A new notion of energy of digraphs, Iran. J. Math. Chem. **12**, 111 (2021).
[95] M. Khan, K. Khan, and S. I. Ahmad, On extremal p-energy of bicyclic digraphs, Polycyclic Aromatic Comp. **42**, 7100 (2022).
[96] V. Nikiforov, The energy of graphs and matrices, J. Math. Anal. Appl. **326**, 1472 (2007).
[97] H. Kharaghani and B. Tayfeh-Rezaie, On the energy of (0, 1)—Matrices, Linear Alg. Appl. **429**, 2046 (2008).
[98] N. Agudelo and J. Rada, Lower bounds of Nikiforov's energy over digraphs, Linear Alg. Appl. **494**, 156 (2016).
[99] J. García, J. Monsalve, and J. Rada, Lower bounds for the spectral norm of digraphs, Linear Alg. Appl. **617**, 151 (2021).
[100] J. Liu and X. Li, Hermitian-adjacency matrices and Hermitian energies of mixed graphs, Linear Alg. Appl. **466**, 182 (2015).
[101] K. Guo and B. Mohar, Hermitian adjacency matrix of digraphs and mixed graphs, J. Graph Theory **85**, 217 (2017).
[102] L. Böttcher and M. A. Porter, Complex networks with complex weights, Phys. Rev. E **109**, 024314 (2024).